Structures and properties the lead-doped carbon clusters $PbC_n/PbC_n^+/PbC_n^-$ ($n=1-10$)

Guoliang Li, Xiaopeng Xing, and Zichao Tang[a)]
State Key Laboratory of Molecular Reaction Dynamics, The Center for Molecular Sciences, Institute of Chemistry, Chinese Academy of Sciences, Beijing 100080, China

(Received 8 November 2002; accepted 21 January 2003)

A systemic density functional theory study of the lead-doped carbon clusters $PbC_n/PbC_n^+/PbC_n^-$ ($n=1-10$) has been carried out using B3LYP method with both CEP-31G and TZP+ basis sets. For each species, the electronic states, relative energies and geometries of various isomers are reported. According to these calculations, the Pb-terminated linear or quasilinear isomer is the most stable structure for $PbC_n/PbC_n^+/PbC_n^-$ clusters except for PbC_2/PbC_2^+ and PbC_{10}/PbC_{10}^+. Both PbC_2 and PbC_2^+ have bent ground state structure. For neutral PbC_{10}, the global minimum possesses a Pb-containing 11-membered ring structure, while for cationic PbC_{10}^+, the Pb-side-on C_{10} monocyclic configuration has lowest energy. Except for the smallest PbC, PbC^+, and PbC^-, the electronic ground state is alternate between $^3\Sigma$ (for *n*-odd member) and $^1\Sigma$ (for the *n*-even member) for linear PbC_n and invariably $^2\Pi$ for linear PbC_n^+ and PbC_n^-. The incremental binding energy diagrams show that strong even–odd alternations in the cluster stability exist for both neutral PbC_n and anionic PbC_n^-, with their *n*-even members being much more stable than the corresponding odd $n-1$ and $n+1$ ones, while for cationic PbC_n^+, the alternation effect is less pronounced. These parity effects also reflect in the ionization potential and electron affinity curves. The even–odd alternation predicted by theoretical studies for anionic PbC_n^- is in good agreement with the even–odd alternation mass distribution observed in the time-of-flight mass spectra. By comparing with the fragmentation energies accompanying various channels, the most favorable dissociation channel for each kind of the $PbC_n/PbC_n^+/PbC_n^-$ clusters are given. © *2003 American Institute of Physics.* [DOI: 10.1063/1.1559916]

I. INTRODUCTION

Small carbon clusters have attracted much attention in the past decades both experimentally and theoretically for their roles in astrochemistry, in combustion processes, and in the chemical vapor deposition of carbon clusters.[1–3] In the interstellar medium, the reactivity of small carbon clusters is forfeited by quasicollisionless conditions, and carbon takes the highly stable, albeit highly reactive, form of linear chains.[4–6] In these linear carbon chains the atomic orbitals are *sp*-hybridized.[7–9] Some of the carbon chains may be terminated by hydrogen atoms or by other heteroatoms. Addition of heteroatoms provides a means to stabilize the carbon chain. The heteroatom-doped carbon clusters containing a first-or second-row element of the Periodic Table have been the subject of numerous studies,[10–58] but few works have concerned heavy-atom-doped carbon clusters. Herein a theoretical investigation on the lead-doped carbon clusters is reported. As the heaviest member of the IVA elements, lead belongs to the same group in the Periodic Table as carbon and silicon. While the silicon-doped carbon clusters have been extensively investigated,[10,16,20,21,27,29,32–58] studies for the lead-doped carbon clusters have not been found in the literature to date to our knowledge.

Theoretical calculations on the system containing heavy atom, such as lead, are very difficult because there are too many electrons. As we know, the complexity of quantum chemical calculations rapidly increases with the number of electrons. In addition, heavy atoms all have very large relativistic effects. To reduce molecular calculations to a computationally more feasible valence electron problem, a common way is the utilization of the relativistic effective core potentials (RECPs), which are usually derived from relativistic Hartree–Fock[59] or Dirac–Fock[60] atomic wave functions and therefore incorporate relativistic effects in the potentials. Because the molecular properties are always ascribed to valence electrons, RECPs replace the chemical inert core electrons with potentials and thus eliminate these core electrons from the molecular calculations. Considering the computational efficiency, RECPs have been well documented by their applications to heavy atom systems, including lead-containing complexes.[61–69] In this article, employing two types of RECPs for lead atom, we present a systemic investigation on the lead-doped carbon clusters $PbC_n/PbC_n^+/PbC_n^-$ ($n=1-10$). The study includes the structures, stability, ionization potentials (IPs), electronic affinities (EAs), and fragmentation energies of the $PbC_n/PbC_n^+/PbC_n^-$ clusters.

II. THEORETICAL METHODS

The $PbC_n/PbC_n^+/PbC_n^-$ clusters were examined using density functional theory (DFT) method at the B3LYP level

a)Author to whom correspondence should be addressed. Electronic mail: zichao@mrdlab.icas.ac.cn

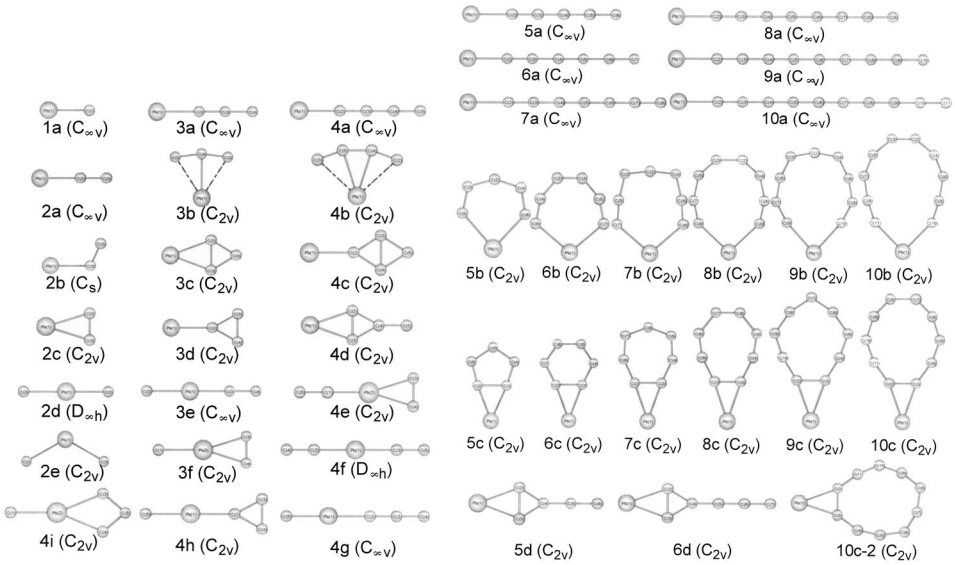

FIG. 1. The structures investigated for the $PbC_n/PbC_n^+/PbC_n^-$ clusters.

of theory, where B3LYP was formed from Becke's three-parameter nonlocal exchange functional[70] along with the Lee, Yang, and Parr nonlocal correlation functional.[71] The DFT/B3LYP method has been successfully applied to many medium-sized heteroatom-doped carbon clusters.[21–31]

Two types of basis sets were used in both geometry optimization and frequency calculations. The first type of basis set, labeled as CEP-31G, employing the effective core potentials (ECPs) developed by Stevens/Basch/Krauss/Jasien and their corresponding valence Gaussian basis for both C and Pb atoms.[72,73] The ECPs retained the outer ns^2np^2 (C, $2s^22p^2$; Pb, $6s^26p^2$) shells in molecular calculations, explicitly replacing the remaining chemically inert core electrons with potentials. For Pb atom, relativistic effects were incorporated by deriving the ECPs from numerical Dirac–Fock atomic wave functions.[60] The contraction schemes used for the basis sets were $(4s4p)/[2s2p]$ for C and $(5s5p)/[2s2p]$ for Pb.

In the second type of basis set, the relativistic effective core potentials (RECPs) given by Hay/Wadt and the corresponding LanL2DZ basis sets were used for Pb atom.[74] The RECPs replaced the inner $1s^22s^22p^63s^23p^63d^{10}4s^24p^64d^{10}4f^{14}5s^25p^65d^{10}$ electrons of the Pb atom by potentials, leaving the remaining $6s^26p^2$ electrons for calculations. The LanL2DZ basis sets were extended by additional two *s*-, two *p*-, and one *d*-type functions in this study.[63] For C atom, all-electron 6-311 +G* basis sets were used, which employed the standard 6-311G triple-split-valence basis sets[75] augmented with *d*-type polarization functions and diffuse *sp*-type functions. This type of basis set is referred as TZVP+ in the present paper.

All calculations were carried out with GAUSSIAN 98 program suite.[76] The spin-restricted wave functions were used for all closed shell systems, and the spin-unrestricted references were employed for the open-shell species. The default integration grid (75, 302) of GAUSSIAN 98 was mainly applied, but we also used the finer grid (99, 590) to check some suspicious results when necessary.

III. RESULTS AND DISCUSSION

Figure 1 gives the structures investigated here for the $PbC_n/PbC_n^+/PbC_n^-$ clusters. We initially optimize these structures at the B3LYP/CEP-31G level of calculations. The obtained geometries are refined with the B3LYP/TZVP+ method. Tables I and II list the optimized geometries and their relative energies, respectively, with the TZVP+ basis set, while the corresponding data with CEP-31G basis set are not shown in this paper; requirement for those data can be supplied by authors. The results show that the calculations with two types of basis sets predict similar energy order for different isomers of the $PbC_n/PbC_n^+/PbC_n^-$ clusters. On the other hand, the B3LYP/CEP-31G calculations usually give longer bond distances and lower relative energies, with respect to the B3LYP/TZVP+ ones. Since the CEP-31G basis set does not consist of the *d*-type polarization functions and diffuse *sp*-type functions, which are necessary for the calculations including ions, in the following discussion, we will mainly use the TZVP+ results, unless otherwise indicated.

A. Structures and energies

The neutral PbC molecule has a triplet $^3\Pi$ ground state with a valence electronic configuration of $\{\text{core}\}\sigma^2\sigma^2\sigma^1\pi^3$. The quintuplet $^5\Pi$ state and the singlet $^1\Delta$ state of the PbC molecule are energetically less stable than the ground $^3\Pi$ state by 21.6 and 22.9 kcal/mol, respectively. Our B3LYP/TZVP+ calculations predict that the equilibrium bond lengths for PbC in its $^3\Pi$, $^5\Pi$, and $^1\Delta$ state are 2.063, 2.182, and 2.335 Å, respectively.

The isomers of the neutral PbC_2 clusters can take the following five possible structures: Pb-terminated linear structure in $C_{\infty v}$ symmetry (**2a**) and bent structure in C_s symme-

TABLE I. Optimized geometries for possible structures of the $PbC_n^{(\pm)}$ clusters at the B3LYP/TZVP+ level of theory. Bond distances and bond angles are in Å and degrees, respectively.

			Neutral				Cation				Anion			
Cluster	Structure	Coordinate[a]	State	Geometry	State	Geometry	State	Geometry	State	Geometry	State	Geometry	State	Geometry
$PbC^{(\pm)}$	**1a** ($C_{\infty v}$)	R_{12}	$^1\Delta$	2.182	$^3\Pi$	2.063	$^2\Delta$	2.191	$^4\Sigma$	2.179	$^2\Sigma$	2.013	$^4\Sigma$	2.213
$PbC_2^{(\pm)}$	**2a** ($C_{\infty v}$)	R_{12}	$^1\Sigma$	2.011	$^3\Pi$	2.187	$^2\Sigma$	2.121	$^4\Sigma$	2.399	$^2\Pi$	2.096	$^4\Sigma$	2.287
		R_{23}		1.278		1.237		1.232		1.298		1.268		1.247
	2b (C_s)	R_{12}	$^1A'$	[b]		[b]	$^2A'$	2.224		[c]		[c]		[c]
		R_{23}						1.265						
		A_{123}						87.3						
	2c (C_{2v})	R_{12}	$^1A_1$	2.187	$^3B_2$	2.394	$^2A_1$	2.338	$^4A_2$	2.690	$^2B_2$	2.306	$^4A_2$	2.630
		R_{23}		1.271		1.282		1.267		1.347		1.286		1.270
$PbC_3^{(\pm)}$	**3a** ($C_{\infty v}$)	R_{12}	$^1\Delta$	2.097	$^3\Sigma$	2.084	$^2\Pi$	2.198	$^4\Sigma$	2.123	$^2\Pi$	2.044	$^4\Pi$	2.205
		R_{23}		1.288		1.286		1.260		1.289		1.316		1.285
		R_{34}		1.303		1.305		1.332		1.269		1.286		1.315
	3b (C_{2v})	R_{12}	$^1A_1$	2.260	$^3B_1$	2.301	$^2B_2$	2.465	$^4B_1$	2.483	$^2A_2$	2.198	$^4A_1$	2.430
		R_{14}		1.329		1.332		1.315		1.308		1.347		1.324
		R_{24}		2.464		2.352		2.483		2.422		2.437		2.525
	3c (C_{2v})	R_{12}	$^1A_1$	2.198	$^3B_1$	2.371	$^2A_1$	2.317		2.342	$^2B_1$	2.274	$^4B_2$	2.346
		R_{23}		1.454		1.520		1.519		1.922		1.451		1.945
		R_{24}		1.431		1.350		1.350		1.385		1.421		1.357
	3d (C_{2v})	R_{12}	$^1A_1$	2.116	$^3B_1$	2.235	$^2A_1$	2.207	$^4A_2$	2.329	$^2B_1$	2.155	$^4A_2$	2.415
		R_{23}		1.428		1.382		1.397		1.405		1.433		1.361
		R_{34}		1.379		1.493		1.458		1.341		1.377		1.549
$PbC_4^{(\pm)}$	**4a** ($C_{\infty v}$)	R_{12}	$^1\Sigma$	2.023	$^3\Sigma$	2.215	$^2\Pi$	2.136	$^4\Pi$	2.378	$^2\Pi$	2.103	$^4\Pi$	2.307
		R_{23}		1.264		1.255		1.258		1.287		1.252		1.262
		R_{34}		1.311		1.321		1.309		1.285		1.342		1.327
		R_{45}		1.272		1.288		1.303		1.336		1.259		1.282
	4b (C_{2v})	R_{12}	$^1A_1$	2.545	$^3A_2$	2.661	$^2B_2$	2.500	$^4A_2$	3.113	$^2B_1$	2.750	$^4A_2$	4.177
		R_{14}		2.343		2.779		2.639		3.038		2.480		3.811
		R_{24}		1.267		1.270		1.267		1.237		1.262		1.275
		R_{45}		1.386		1.342		1.352		1.355		1.377		1.335
	4c (C_{2v})	R_{12}	$^1A_1$	2.079	$^3A_2$	2.264	$^2B_1$	2.216	$^4B_2$	2.187	$^2B_2$	2.133	$^4A_1$	2.209
		R_{23}		1.440		1.427		1.416		1.444		1.450		1.434
		R_{34}		1.479		1.496		1.508		1.765		1.477		1.702
		R_{45}		1.431		1.446		1.457		1.385		1.430		1.461
	4d (C_{2v})	R_{12}	$^1A_1$	2.184	$^3A_2$	2.248	$^2B_1$	2.290	$^4A_2$	2.288	$^2B_2$	2.271	$^4B_2$	2.441
		R_{23}		1.382		1.439		1.411		1.475		1.373		1.395
		R_{24}		1.461		1.426		1.415		1.384		1.499		1.437
		R_{45}		1.298		1.371		1.356		1.383		1.290		1.357
$PbC_5^{(\pm)}$	**5a** ($C_{\infty v}$)	R_{12}	$^1\Delta$	2.083	$^3\Sigma$	2.079	$^2\Pi$	2.161	$^4\Sigma$	2.113	$^2\Pi$	2.041	$^4\Pi$	2.188
		R_{23}		1.284		1.272		1.250		1.268		1.299		1.263
		R_{34}		1.287		1.288		1.311		1.289		1.271		1.308
		R_{45}		1.290		1.288		1.263		1.298		1.317		1.295
		R_{56}		1.289		1.291		1.315		1.246		1.273		1.291
	5b (C_{2v})	R_{15}	$^1A_1$	2.417	$^3B_1$	2.382	$^2B_1$	2.418	$^4A_2$	2.393	$^2B_1$	2.360	$^4A_1$	2.694
		R_{53}		1.270		1.271		1.272		1.289		1.277		1.275
		R_{32}		1.372		1.342		1.309		1.337		1.370		1.355
		A_{153}		90.5		93.8		130.0		113.6		92.7		76.9
		A_{532}		167.3		155.6		113.6		153.3		165.8		166.7
	5c (C_{2v})	R_{12}	$^1A_1$	2.194		[d]		[d]	$^4B_1$	2.208	$^2B_2$	2.147	$^4B_2$	2.144
		R_{23}		1.957						1.477		1.560		1.637
		R_{34}		1.318						1.460		1.387		1.365
		R_{45}		1.366						1.325		1.368		1.404
		A_{234}		82.0						108.3		104.3		104.3
	5d (C_{2v})	R_{12}	$^1A_1$	2.196	$^3A_2$	2.368	$^2A_1$	2.273	$^4B_1$	2.412	$^2B_1$	2.282	$^4B_2$	2.332
		R_{23}		1.448		1.389		1.478		1.351		1.445		1.834
		R_{24}		1.409		1.412		1.373		1.432		1.395		1.393
		R_{45}		1.336		1.331		1.382		1.328		1.366		1.397
		R_{56}		1.267		1.286		1.211		1.239		1.254		1.247
$PbC_6^{(\pm)}$	**6a** ($C_{\infty v}$)	R_{12}	$^1\Sigma$	2.035	$^3\Sigma$	2.197	$^2\Pi$	2.120	$^4\Pi$	2.284	$^2\Pi$	2.113	$^4\Pi$	2.240
		R_{23}		1.264		1.248		1.252		1.270		1.251		1.262
		R_{34}		1.302		1.321		1.312		1.290		1.331		1.316
		R_{45}		1.255		1.251		1.257		1.282		1.243		1.259
		R_{56}		1.305		1.309		1.296		1.277		1.334		1.317

TABLE I. (*Continued*.)

			Neutral				Cation				Anion			
Cluster	Structure	Coordinate[a]	State	Geometry	State	Geometry	State	Geometry	State	Geometry	State	Geometry	State	Geometry
		R_{67}		1.274		1.286		1.301		1.324		1.261		1.280
	6b (C_{2v})	R_{16}	$^1A_1$	2.307	$^3B_2$	2.273	$^2A_1$	2.371	$^4A_2$	2.386	$^2B_1$	2.513	$^4A_2$	2.441
		R_{46}		1.254		1.255		1.261		1.263		1.252		1.257
		R_{24}		1.346		1.346		1.323		1.324		1.364		1.361
		R_{23}		1.243		1.372		1.259		1.417		1.236		1.356
		A_{164}		118.0		125.3		134.3		128.9		109.3		113.7
		A_{642}		151.2		158.8		137.8		157.3		152.2		164.6
	6c (C_{2v})	R_{12}	$^1A'$	2.200	$^3A'$	2.200	$^2A'$	2.281	$^4A'$	2.245	$^2A'$	2.176	$^4A'$	2.202
		R_{23}		1.484		1.463		1.450		1.536		1.478		1.396
		R_{34}		1.372		1.364		1.347		1.316		1.367		1.396
		R_{45}		1.286		1.380		1.313		1.347		1.318		1.382
		R_{56}		1.312		1.402		1.287		1.428		1.436		1.366
	6d (C_{2v})	R_{12}	$^1A_1$	2.195	$^3A_2$	2.228	$^2B_1$	2.271	$^4A_2$	2.263	$^2B_2$	2.215	$^4B_2$	2.350
		R_{23}		1.405		1.451		1.430		1.463		1.423		1.426
		R_{24}		1.435		1.409		1.399		1.388		1.442		1.407
		R_{45}		1.293		1.337		1.332		1.355		1.306		1.343
		R_{56}		1.290		1.273		1.260		1.269		1.305		1.285
		R_{67}		1.284		1.313		1.319		1.272		1.283		1.305
$PbC_7^{(\pm)}$	**7a** ($C_{\infty v}$)	R_{12}	$^1\Delta$	2.076	$^3\Sigma$	2.076	$^2\Pi$	2.139	$^4\Sigma$	2.105	$^2\Pi$	2.043	$^4\Pi$	2.176
		R_{23}		1.269		1.268		1.248		1.261		1.291		1.255
		R_{34}		1.294		1.294		1.317		1.300		1.278		1.318
		R_{45}		1.274		1.273		1.249		1.275		1.299		1.270
		R_{56}		1.274		1.275		1.296		1.268		1.260		1.284
		R_{67}		1.295		1.293		1.270		1.310		1.320		1.305
		R_{78}		1.285		1.287		1.308		1.237		1.270		1.282
	7b (C_{2v})	R_{17}	$^1A_1$	2.301	$^3B_1$	2.283	$^2A_2$	2.346	$^4B_1$	2.354	$^2B_1$	2.267	$^4B_2$	2.418
		R_{75}		1.254		1.255		1.256		1.270		1.263		1.260
		R_{53}		1.369		1.350		1.315		1.328		1.377		1.353
		R_{32}		1.297		1.289		1.288		1.297		1.304		1.290
		A_{175}		123.5		130.3		149.4		139.2		117.1		126.1
		A_{753}		172.3		163.7		141.4		158.9		174.6		162.4
		A_{532}		109.9		121.6		151.9		117.4		109.2		124.9
	7c (C_{2v})	R_{12}	$^1A_1$	2.228	$^3B_1$	2.245	$^2A_1$	2.283	$^4A_2$	2.420	$^2B_1$	2.265	$^4B_2$	2.351
		R_{23}		1.447		1.475		1.483		1.347		1.468		3.217
		R_{34}		1.372		1.354		1.342		1.376		1.372		1.264
		R_{45}		1.280		1.260		1.262		1.271		1.297		1.319
		R_{56}		1.319		1.380		1.368		1.335		1.394		1.351
		A_{234}		114.4		115.0		115.8		125.8		118.3		85.5
		A_{345}		153.9		146.5		144.7		123.8		126.0		159.3
$PbC_8^{(\pm)}$	**8a** ($C_{\infty v}$)	R_{12}	$^1\Sigma$	2.040	$^3\Sigma$	2.184	$^2\Pi$	2.110	$^4\Pi$	2.230	$^2\Pi$	2.119	$^4\Pi$	2.193
		R_{23}		1.264		1.246		1.250		1.262		1.250		1.263
		R_{34}		1.302		1.325		1.316		1.298		1.330		1.311
		R_{45}		1.256		1.246		1.250		1.274		1.243		1.262
		R_{56}		1.296		1.309		1.298		1.275		1.323		1.303
		R_{67}		1.258		1.255		1.262		1.284		1.244		1.261
		R_{78}		1.304		1.306		1.292		1.276		1.330		1.315
		R_{89}		1.275		1.285		1.298		1.316		1.262		1.278
	8b (C_{2v})	R_{18}	$^1A_1$	2.297	$^3A_2$	2.337	$^2B_2$	2.357	$^4A_1$	2.358	$^2B_1$	2.384	$^4A_2$	2.299
		R_{86}		1.233		1.257		1.243		1.277		1.244		1.259
		R_{64}		1.370		1.326		1.341		1.295		1.359		1.349
		R_{42}		1.226		1.259		1.244		1.298		1.265		1.316
		R_{23}		1.373		1.325		1.337		1.275		1.372		1.273
		A_{186}		140.3		150.3		150.7		153.3		137.2		141.3
		A_{864}		158.2		150.9		152.6		151.7		156.3		168.1
		A_{642}		144.4		149.2		147.3		146.0		149.4		123.6
	8c (C_{2v})	R_{12}	$^1A_1$	2.200	$^3A_2$	2.183	$^2A_1$	2.233	$^4B_2$	2.260	$^2A_2$	2.181	$^4B_1$	2.184
		R_{23}		1.379		1.492		1.400		1.511		1.472		1.497
		R_{34}		1.426		1.347		1.400		1.324		1.368		1.360
		R_{45}		1.227		1.271		1.239		1.287		1.262		1.259
		R_{56}		1.409		1.351		1.374		1.328		1.388		1.357
		A_{234}		1.225		1.259		1.239		1.274		1.246		1.390
		A_{345}		117.4		118.1		118.6		117.9		116.8		116.5
		A_{456}		160.3		161.8		160.0		162.4		163.3		153.0

TABLE I. (*Continued*.)

			Neutral				Cation				Anion			
Cluster	Structure	Coordinate[a]	State	Geometry	State	Geometry	State	Geometry	State	Geometry	State	Geometry	State	Geometry
$PbC_9^{(\pm)}$	**9a** ($C_{\infty v}$)	R_{12}	$^1\Delta$	2.072	$^3\Sigma$	2.074	$^2\Pi$	2.125	$^4\Sigma$	2.100	$^2\Pi$	2.048	$^4\Pi$	2.168
		R_{23}		1.267		1.266		1.247		1.258		1.285		1.251
		R_{34}		1.297		1.298		1.319		1.305		1.284		1.324
		R_{45}		1.269		1.268		1.246		1.265		1.291		1.258
		R_{56}		1.281		1.282		1.303		1.281		1.266		1.297
		R_{67}		1.280		1.279		1.256		1.287		1.304		1.281
		R_{78}		1.269		1.271		1.290		1.257		1.256		1.274
		R_{89}		1.297		1.295		1.273		1.318		1.321		1.309
		$R_{9,10}$		1.283		1.284		1.304		1.232		1.269		1.278
	9b (C_{2v})	R_{19}	$^1A_1$	2.239	$^3B_1$	2.278	$^2B_1$	2.334	$^4A_2$	2.321	$^2B_1$	2.234	$^4B_2$	2.427
		R_{97}		1.257		1.247		1.247		1.262		1.257		1.246
		R_{75}		1.314		1.336		1.321		1.315		1.331		1.348
		R_{53}		1.277		1.257		1.270		1.271		1.263		1.252
		R_{32}		1.297		1.315		1.297		1.313		1.315		1.332
		A_{197}		162.6		147.5		161.1		153.9		147.5		144.5
		A_{975}		148.2		162.7		148.9		164.8		162.5		161.5
		A_{753}		162.7		148.2		162.8		144.8		147.5		152.6
		A_{532}		124.9		151.3		125.4		158.9		152.2		152.4
	9c (C_{2v})	R_{12}	$^1A_1$	2.194	$^3B_2$	2.188	$^2B_1$	2.285	$^4B_1$	2.237	$^2B_2$	2.182	$^4A_2$	2.331
		R_{23}		1.453		1.480		1.487		1.418		1.441		1.432
		R_{34}		1.325		1.329		1.299		1.367		1.355		1.322
		R_{45}		1.284		1.275		1.304		1.254		1.261		1.281
		R_{56}		1.301		1.317		1.288		1.336		1.337		1.323
		R_{67}		1.301		1.299		1.307		1.297		1.294		1.305
		A_{234}		121.9		122.9		121.6		122.0		123.5		124.4
		A_{345}		167.1		155.8		167.7		157.6		157.5		154.5
		A_{456}		124.5		154.6		123.9		154.2		127.0		154.8
$PbC_{10}^{(\pm)}$	**10a** ($C_{\infty v}$)	R_{12}	$^1\Sigma$	2.046	$^3\Sigma$	2.181	$^2\Pi$	2.103	$^4\Pi$	2.196	$^2\Pi$	2.123	$^4\Pi$	2.160
		R_{23}		1.264		1.243		1.249		1.257		1.250		1.264
		R_{34}		1.303		1.330		1.318		1.304		1.329		1.308
		R_{45}		1.257		1.241		1.247		1.267		1.243		1.264
		R_{56}		1.295		1.316		1.304		1.280		1.322		1.298
		R_{67}		1.259		1.249		1.256		1.281		1.245		1.265
		R_{78}		1.294		1.306		1.293		1.270		1.319		1.301
		R_{89}		1.259		1.255		1.265		1.284		1.246		1.261
		$R_{9,10}$		1.303		1.305		1.291		1.277		1.326		1.314
		$R_{10,11}$		1.276		1.283		1.296		1.310		1.263		1.277
	10b (C_{2v})	$R_{1,10}$	$^1A_1$	2.242	$^3B_2$	2.243	$^2A_1$	2.301	$^4A_2$	2.332	$^2B_2$	2.346	$^4B_2$	2.350
		$R_{10,8}$		1.241		1.245		1.247		1.250		1.243		1.245
		R_{86}		1.338		1.329		1.323		1.318		1.346		1.340
		R_{64}		1.238		1.251		1.253		1.265		1.238		1.246
		R_{42}		1.339		1.324		1.311		1.299		1.354		1.342
		R_{23}		1.241		1.365		1.258		1.396		1.236		1.357
		$A_{1,10,8}$		153.7		151.7		163.0		152.8		154.4		151.5
		$A_{10,8,6}$		166.0		165.6		158.1		165.4		163.2		164.1
		A_{864}		157.2		158.6		158.8		157.6		160.9		161.7
		A_{642}		146.5		164.7		143.5		164.9		143.4		164.3
	10c (C_{2v})	R_{12}	$^1A_1$	2.211	$^3A_2$	2.457	$^2B_2$	2.288	$^4A_2$	2.567	$^2B_1$	2.309	$^4A_2$	2.369
		R_{23}		1.431		1.375		1.406		1.397		1.434		1.382
		R_{34}		1.348		1.308		1.324		1.299		1.334		1.330
		R_{45}		1.250		1.275		1.268		1.276		1.265		1.267
		R_{56}		1.323		1.296		1.296		1.304		1.319		1.321
		R_{67}		1.253		1.276		1.275		1.264		1.262		1.345
		A_{234}		1.334		1.302		1.297		1.318		1.348		1.253
		A_{345}		126.1		130.3		127.7		131.2		124.0		127.7
		A_{456}		161.5		160.4		163.4		155.7		167.2		160.2
		A_{567}		148.8		142.0		141.7		151.1		141.9		158.9

[a]Atom numbering is shown in Fig. 1.
[b]Converging to **2c**.
[c]Converging to **2a**.
[d]Converging to **5b**.

TABLE II. Relative energies (E_{rel}, in kcal/mol) and numbers of imaginary vibrational frequencies (N_{imag}, given in parentheses) for the possible structures of the $PbC_n^{(\pm)}$ clusters at the B3LYP level with the TZVP+ basis sets.

		Neutral				Cation				Anion			
Cluster	Structure	State	E_{rel} (N_{imag})	State	E_{rel} (N_{imag})	State	E_{rel} (N_{imag})	State	E_{rel} (N_{imag})	State	E_{rel} (N_{imag})	State	E_{rel} (N_{imag})
$PbC^{(\pm)}$	**1a** ($C_{\infty v}$)	$^1\Delta$	22.9 (0)	$^3\Pi$	**0.0** (0)	$^2\Delta$	13.1 (0)	$^4\Sigma$	**0.0** (0)	$^2\Sigma$	**0.0** (0)	$^4\Sigma$	25.0 (0)
$PbC_2^{(\pm)}$	**2a** ($C_{\infty v}$)	$^1\Sigma$	0.0 (2)	$^3\Pi$	35.5 (0)	$^2\Sigma$	0.0 (0)	$^4\Sigma$	61.7 (0)	$^2\Pi$	**0.0** (0)	$^4\Sigma$	37.7 (0)
	2b (C_s)	$^1A'$	[a]		[a]	$^2A'$	**−0.6** (0)		[b]		[b]		[b]
	2c (C_{2v})	$^1A_1$	**−2.3** (0)	$^3B_2$	32.3 (0)	$^2A_1$	−0.5 (1)	$^4A_2$	67.1 (0)	$^2B_2$	4.0 (0)	$^4A_2$	41.2 (0)
	2d ($D_{\infty h}$)	$^1\Sigma_g$	172.9 (0)	$^3\Sigma_u$	168.8 (0)	$^2\Pi_u$	179.4 (0)	$^4\Pi_g$	168.2 (1)	$^2\Pi_g$	142.8 (0)	$^4\Sigma_u$	144.2 (0)
	2e (C_{2v})		[c]		[c]	$^2B_1$	177.3 (0)	$^4B_2$	162.7 (0)		[d]		[d]
$PbC_3^{(\pm)}$	**3a** ($C_{\infty v}$)	$^1\Delta$	13.2 (0)	$^3\Sigma$	**0.0** (0)	$^2\Pi$	**0.0** (0)	$^4\Sigma$	19.9 (0)	$^2\Pi$	**0.0** (0)	$^4\Pi$	16.4 (1)
	3b (C_{2v})	$^1A_1$	9.7 (0)	$^3B_1$	15.6 (0)	$^2B_2$	8.5 (0)	$^4B_1$	57.5 (1)	$^2A_2$	21.5 (1)	$^4A_1$	26.3 (0)
	3c (C_{2v})	$^1A_1$	13.9 (0)	$^3B_1$	19.7 (0)	$^2A_1$	1.1 (0)	$^4A_2$	79.7 (2)	$^2B_1$	17.4 (0)	$^4B_2$	52.6 (1)
	3d (C_{2v})	$^1A_1$	25.4 (1)	$^3B_1$	38.6 (0)	$^2A_1$	27.9 (0)	$^4A_2$	38.5 (0)	$^2B_1$	21.3 (0)	$^4A_2$	42.7 (1)
	3e ($C_{\infty v}$)	$^1\Delta$	130.8 (1)	$^3\Sigma$	104.6 (2)	$^2\Pi$	144.0 (2)	$^4\Sigma$	130.6 (2)	$^2\Pi$	87.2 (0)	$^4\Sigma$	104.9 (4)
	3f (C_{2v})	$^1A_1$	129.3 (0)	$^3A_2$	102.5 (0)	$^2A_2$	140.0 (3)	$^4A_2$	131.8 (2)	$^2B_1$	90.3 (0)	$^4B_1$	90.3 (0)
$PbC_4^{(\pm)}$	**4a** ($C_{\infty v}$)	$^1\Sigma$	**0.0** (0)	$^3\Sigma$	30.0 (0)	$^2\Pi$	**0.0** (1)[e]	$^4\Pi$	38.7 (1)	$^2\Pi$	**0.0** (0)	$^4\Pi$	34.4 (0)
	4b (C_{2v})	$^1A_1$	12.3 (0)	$^3A_2$	55.0 (1)	$^2B_2$	26.2 (2)	$^4A_2$	90.5 (2)	$^2B_1$	14.8 (0)	$^4A_2$	68.6 (0)
	4c (C_{2v})	$^1A_1$	53.0 (0)	$^3A_2$	63.8 (0)	$^2B_1$	35.4 (0)	$^4B_2$	81.3 (2)	$^2B_2$	58.5 (0)	$^4A_1$	97.2 (1)
	4d (C_{2v})	$^1A_1$	54.5 (0)	$^3A_2$	81.0 (0)	$^2B_1$	46.9 (0)	$^4A_2$	81.0 (0)	$^2B_2$	69.6 (1)	$^4B_2$	86.8 (0)
	4e (C_{2v})	$^1A_1$	100.4 (2)	$^3B_2$	157.1 (1)	$^2A_1$	131.5 (0)	$^4A_2$	189.0 (0)	$^2B_2$	99.8 (1)	$^4B_2$	127.9 (1)
	4f ($D_{\infty h}$)	$^1\Sigma_g$	101.8 (4)	$^3\Sigma_u$	141.6 (6)	$^2\Sigma_u$	133.9 (3)	$^4\Pi_u$	162.9 (5)	$^2\Sigma_g$	95.5 (6)	$^4\Sigma_g$	132.9 (5)
	4g ($C_{\infty v}$)	$^1\Sigma$	156.3 (0)	$^3\Sigma$	153.2 (2)	$^2\Pi$	143.8 (2)	$^4\Sigma$	133.4 (2)	$^2\Sigma$	142.6 (4)	$^4\Pi$	139.8 (2)
	4h (C_{2v})	$^1A_1$	175.6 (0)	$^3A_2$	161.9 (2)	$^2A_2$	175.3 (2)	$^4A_2$	[f]	$^2B_2$	142.7 (1)	$^4B_2$	167.9 (2)
	4i (C_{2v})	$^1A_1$	181.2 (2)	$^3A_2$	156.5 (2)	$^2A_2$	150.0 (2)	$^4A_2$	140.3 (2)	$^2B_2$	148.0 (1)	$^4A_2$	154.6 (2)
$PbC_5^{(\pm)}$	**5a** ($C_{\infty v}$)	$^1\Delta$	10.7 (0)	$^3\Sigma$	**0.0** (0)	$^2\Pi$	**0.0** (0)	$^4\Sigma$	20.6 (0)	$^2\Pi$	**0.0** (0)	$^4\Pi$	13.2 (0)
	5b (C_{2v})	$^1A_1$	20.7 (0)	$^3B_1$	18.8 (0)	$^2B_1$	29.1 (0)	$^4A_2$	52.8 (0)	$^2B_1$	11.7 (0)	$^4A_1$	40.0 (0)
	5c (C_{2v})	$^1A_1$	52.2 (0)		[g]		[g]	$^4B_1$	96.1 (1)	$^2B_2$	94.1 (0)	$^4B_2$	90.8 (0)
	5d (C_{2v})	$^1A_1$	28.2 (0)	$^3A_2$	52.8 (1)	$^2A_1$	45.6 (1)	$^4B_1$	88.3 (0)	$^2B_1$	25.7 (0)	$^4B_2$	94.1 (2)
$PbC_6^{(\pm)}$	**6a** ($C_{\infty v}$)	$^1\Sigma$	**0.0** (0)	$^3\Sigma$	23.7 (0)	$^2\Pi$	**0.0** (1)[h]	$^4\Pi$	31.2 (0)	$^2\Pi$	**0.0** (0)	$^4\Pi$	30.2 (0)
	6b (C_{2v})	$^1A_1$	12.4 (0)	$^3B_2$	42.0 (0)	$^2A_1$	24.6 (1)	$^4A_2$	51.6 (0)	$^2B_1$	37.3 (1)	$^4A_2$	67.7 (0)
	6c (C_{2v})	$^1A_1$	37.1 (1)	$^3A_1$	55.4 (1)	$^2B_2$	34.0 (1)	$^4A_1$	66.5 (1)	$^2B_2$	63.2 (0)	$^4A_1$	90.8 (1)
	6d (C_{2v})	$^1A_1$	50.8 (0)	$^3A_2$	68.0 (0)	$^2B_1$	43.4 (0)	$^4A_2$	75.2 (0)	$^2B_2$	62.6 (0)	$^4B_2$	74.4 (0)
$PbC_7^{(\pm)}$	**7a** ($C_{\infty v}$)	$^1\Delta$	9.1 (0)	$^3\Sigma$	**0.0** (0)	$^2\Pi$	**0.0** (0)	$^4\Sigma$	20.7 (0)	$^2\Pi$	**0.0** (0)	$^4\Pi$	10.8 (0)
	7b (C_{2v})	$^1A_1$	17.3 (0)	$^3B_1$	22.3 (0)	$^2A_2$	22.5 (0)	$^4B_1$	53.8 (1)	$^2A_2$	27.3 (1)	$^4A_1$	45.2 (0)
	7c (C_{2v})	$^1A_1$	64.5 (4)	$^3B_1$	38.2 (0)	$^2A_1$	23.5 (0)	$^4A_2$	59.5 (1)	$^2B_1$	42.3 (0)	$^4B_2$	55.3 (0)
$PbC_8^{(\pm)}$	**8a** ($C_{\infty v}$)	$^1\Sigma$	**0.0** (0)	$^3\Sigma$	19.5 (0)	$^2\Pi$	**0.0** (0)	$^4\Pi$	26.1 (0)	$^2\Pi$	**0.0** (0)	$^4\Pi$	27.5 (0)
	8b (C_{2v})	$^1A_1$	22.6 (2)	$^3A_2$	49.5 (1)	$^2B_2$	26.0 (1)	$^4A_1$	54.6 (2)	$^2B_1$	39.0 (1)	$^4A_2$	62.7 (1)
	8c (C_{2v})	$^1A_1$	48.1 (2)	$^3A_2$	69.2 (2)	$^2A_1$	45.2 (1)	$^4B_2$	54.9 (1)	$^2A_2$	80.9 (3)	$^4B_1$	86.7 (0)
$PbC_9^{(\pm)}$	**9a** ($C_{\infty v}$)	$^1\Delta$	8.0 (0)	$^3\Sigma$	**0.0** (0)	$^2\Pi$	**0.0** (2)[i]	$^4\Sigma$	20.9 (0)	$^2\Pi$	**0.0** (0)	$^4\Pi$	9.2 (0)
	9b (C_{2v})	$^1A_1$	13.6 (0)	$^3B_1$	13.3 (0)	$^2B_1$	15.6 (0)	$^4A_2$	36.6 (0)	$^2B_1$	15.3 (0)	$^4A_1$	45.8 (0)
	9c (C_{2v})	$^1A_1$	7.5 (0)	$^3B_2$	37.4 (2)	$^2B_1$	22.8 (1)	$^4B_1$	43.5 (1)	$^2B_2$	42.4 (1)	$^4A_2$	63.2 (3)
$PbC_{10}^{(\pm)}$	**10a** ($C_{\infty v}$)	$^1\Sigma$	0.0 (2)[i]	$^3\Sigma$	17.2 (2)[i]	$^2\Pi$	0.0 (2)[i]	$^4\Pi$	22.5 (2)[i]	$^2\Pi$	**0.0** (2)[i]	$^4\Pi$	25.1 (2)[i]
	10b (C_{2v})	$^1A_1$	**−1.8** (0)	$^3B_2$	29.4 (0)	$^2A_1$	9.6 (1)[i]	$^4A_2$	39.9 (0)	$^2B_1$	29.2 (1)	$^4A_2$	59.1 (0)
	10c (C_{2v})	$^1A_1$	−0.7 (1)	$^3A_2$	26.8 (2)	$^2B_2$	−4.2 (1)	$^4A_2$	54.1 (2)	$^2B_1$	31.3 (1)	$^4A_2$	55.0 (0)
	10c-2 (C_s)	$^1A'$	−1.5 (0)	$^3A''$	24.1 (0)	$^2A'$	**−4.2** (0)	$^4A''$	34.6 (0)	$^2A''$	28.3 (0)		

[a]Converging to **2c**.
[b]Converging to **2a**.
[c]Converging to **2c**.
[d]Converging to **2d**.
[e]See the text for the corresponding structure with all real vibrational frequency.
[f]Converging to **4i**.
[g]Converging to **5b**.
[h]See the text for the corresponding structure with all real vibrational frequency.
[i]It has been noted that the 6-311+G* basis sets become over-complete for some carbon chain systems because of the large overlap between the diffuse functions. When we reinvestigate these systems using 6-311G* basis sets (in which diffuse *sp*-functions are excluded) for carbon atoms, they all have no imaginary vibrational frequency, indicating that they should be stable.
[j]Further calculations following the normal mode of the imaginary vibrational frequency lead to a C_s symmetry structure with its relative energy being 9.6 kcal/mol at the B3LYP/TZVP+ level of theory, with respect to the $^2\Pi$ state of **10a**.

try (**2b**), Pb-side-on adduct Pb(C_2) in C_{2v} symmetry (**2c**), and Pb-inserted dicarbide CPbC in $D_{\infty h}$ symmetry (**2d**) and in C_{2v} symmetry (**2e**). At the B3LYP/CEP-31G level of computations, structure **2b** in its singlet $^1A'$ state has lowest energy, while structure **2a** in its $^1\Sigma$ state and structure **2c** in its $^1A_1$ state are energetically less stable by 0.1 and 2.6 kcal/mol, respectively. On the other hand, the B3LYP/TZVP+ calculations predict that the $^1A_1$ state of **2c** has lowest energy with the $^1\Sigma$ state of **2a** being 2.3 kcal/mol energetically higher. The optimization on structure **2b** also converges to **2c** with the B3LYP/TZVP+ method. Since the singlet states of structure **2a**, **2b**, and **2c** are almost energetically degenerate, to further characterize their energies, we also study them at higher CCSD(T) level of theory. The CCSD(T)[77,78] method requests a coupled cluster calculations using both single and double substitutions and including triple excitations. Both the CCSD(T)/CEP-31G and CCSD(T)/TZVP+ calculations predict that the $^1A'$ state of **2b** has lowest energy and all real vibrational frequencies, indicating that the $^1A'$ state (**2b**) should be the ground state of the neutral PbC_2 cluster. The $^1A_1$ state of **2c** and the $^1\Sigma$ state of **2a** lie 0.03 and 5.0 kcal/mol above the $^1A'$ state (**2b**), respectively, with the CCSD(T)/TZVP+ method, and have one or two imaginary vibrational frequencies. Following the normal modes related to these imaginary frequencies, structure **2c** and **2a** in their singlet states also fall into structure **2b**. Compared with their singlet states, the corresponding triplet states of structure **2a**, **2b**, and **2c** all have higher energies. Structure **2d**, either in its singlet $^1\Sigma_g$ state or in its triplet $^3\Sigma_u$ state, has very high energies (see Table II), indicating that the PbC_2 cluster prefers the structures in which the two C atoms bond to each other, with the Pb atom being end-on or side-on the C_2 unit. When we start the Pb-inserted dicarbide structure CPbC with C_{2v} symmetry (**2e**), it goes back to the side-on adduct structure Pb(C_2) (**2c**).

Various possible structures of the neutral PbC_3 cluster have been investigated: the linear structures with Pb atom located at one end (PbCCC, **3a**) or in a central position (CPbCC, **3e**), the Pb(C_3) structures with Pb atom bonded to one side of a quasilinear C_3 unit (**3b**), or to one side of a cyclic C_3 unit (**3c**), or to one apex of a cyclic C_3 unit (**3d**), and structure **3d**'s analogue (**3f**) in which the Pb atom taking part in the ring and a C atom in an exocyclic position, ... The global minimum for neutral PbC_3 is the $C_{\infty v}$ symmetry linear structure PbCCC (**3a**) in its triplet $^3\Sigma$ state. The calculated bond distances for structure **3a** are R(Pb1–C2)=2.084, R(C2–C3)=1.286, and R(C3–C4)=1.305 Å with the B3LYP/TZVP+ method. Compared with the $^3\Sigma$ ground state, the corresponding singlet $^1\Delta$ state of **3a** is 13.2 kcal/mol energetically less stable. Another low-energy minimum found for PbC_3 is structure **3b**. Its singlet $^1A_1$ state and triplet $^3B_1$ state are energetically above the $^3\Sigma$ ground state (**3a**) by 9.7 and 15.6 kcal/mol, respectively, at the B3LYP/TZVP+ level. Structure **3c** is also a minimum on the potential energy surface (PES) of the PbC_3 cluster. It has similar electronic states ($^1A_1$ and $^3B_1$) to structure **3b**, but is about 4.1 kcal/mol less stable than the latter, for both its singlet and triplet states. Structure **3d** is either a saddle point or a minimum on the PES of PbC_3, with its singlet $^1A_1$ and triplet $^3B_1$ state energetically higher than the $^3\Sigma$ ground state (**3a**) by 25.4 and 38.6 kcal/mol, respectively. For the structures in which three C atoms are separated, such as **3e** and **3f**, they both have very high energies, lying more than 100 kcal/mol above the $^3\Sigma$ ground state (**3a**), so we do not consider this kind of structures further. We have also studied the C_{3v} symmetry trigonal pyramid structure of PbC_3. It is about 64 kcal/mol energetically less stable than the $^3\Sigma$ ground state (**3a**), and has two imaginary vibrational frequencies, expressing it is not a minimum on the PES of PbC_3.

Attaching a C atom to the structures mentioned above for PbC_3 leads to the possible structures of PbC_4 investigated herein, as depicted in Fig. 1. For the neutral PbC_4 cluster, the most stable isomer possesses a linear PbCCCC structure (**4a**). Its electronic ground state has $^1\Sigma$ symmetry. The calculated bond distances are R(Pb1–C2)=2.023, R(C2–C3)=1.264, R(C3–C4)=1.311, and R(C4–C5)=1.272 Å at the B3LYP/TZVP+ level of calculations. When starting from a Pb-containing monocyclic structure of PbC_4 with C_{2v} symmetry, we get a fanlike structure (**4b**), which can be viewed as a Pb atom bonded to one side of a chain C_4 unit. Structure **4b** in its lowest-lying $^1A_1$ state has all real vibrational frequencies and lies only 12.3 kcal/mol energetically above the $^1\Sigma$ ground state (**4a**) with the B3LYP/TZVP+ method. Kitelike structures **4c** and **4d**, which can be yielded by adding a C atom to structure **3d** or **3c**, are also minima on the PES of PbC_4, with their energies higher than the global minimum by 53.0 and 54.5 kcal/mol, respectively, at the B3LYP/TZVP+ level. The structures with the Pb atom bonded to four-membered ring C_4 unit from its one side (in C_{2v} symmetry) or from its top (in C_{4v} symmetry) are also investigated. In their singlet states, the former transforms into the fanlike planar structure (**4b**), while the latter has very high energy. Again, for the structures in which four C atoms are separated by the Pb atom, such as **4e**, **4f**, **4g**, **4h**, and **4i**, they all have very high energies, lying more than 100 kcal/mol above the ground $^1\Sigma$ state (**4a**).

There are mainly four kinds of structures investigated for the PbC_5 cluster, i.e., linear PbCCCCC structure (**5a**), Pb-containing monocyclic ring (**5b**), Pb-side-on C_5 monocyclic ring (**5c**), and kitelike structure (**5d**). For PbC_n, when the n carbon atoms are inserted by the lead atom, the structures all have very high energies, such as **2d–2e**, **3e–3f**, **4e–4i**, so we do not consider this kind of structures further when $n \geqslant 5$. The ground state of the neutral PbC_5 cluster is the triplet $^3\Sigma$ state of structure **5a**. Its corresponding singlet $^1\Delta$ state is higher in energy by 10.7 kcal/mol at the B3LYP/TZVP+ level. The calculated bond distances for the ground state are R(Pb1–C2)=2.079, R(C2–C3)=1.272, R(C3–C4)=1.288, R(C4–C5)=1.288, and R(C5–C6)=1.291 Å. Structure **5b** is also a minimum on the PES of PbC_5, with its lowest triplet electronic state ($^3B_1$) being 18.8 kcal/mol energetically less stable than the $^3\Sigma$ ground state. Structure **5c** either converges to structure **5b**, or has very high energy, indicating it is unstable. The kitelike structure (**5d**) is a minimum in its lowest-lying singlet $^1A_1$ state, with its energy being 28.2 kcal/mol higher than the $^3\Sigma$ ground state (**5a**).

For the PbC_6 cluster, we also mainly investigate its four

types of structures: (**6a**) the linear structure with the Pb atom located at one end; (**6b**) the Pb-containing seven-membered ring structure; (**6c**) the structure with the Pb atom bonded to one side of a monocyclic C_6 unit; and (**6d**) the kite-like structure. Similar to that of PbC_5, the global minimum of the neutral PbC_6 cluster also has a linear PbCCCCCC structure (**6a**), but its electronic ground state is its singlet $^1\Sigma$ state. Our B3LYP/TZVP+ calculation predicts the bond distances for the ground state are $R(\mathrm{Pb1-C2})=2.035$, $R(\mathrm{C2-C3})=1.264$, $R(\mathrm{C3-C4})=1.302$, $R(\mathrm{C4-C5})=1.255$, $R(\mathrm{C5-C6})=1.305$, and $R(\mathrm{C6-C7})=1.274$ Å, respectively. Structure **6b** in its singlet $^1A_1$ is either a minimum (at the B3LYP/TZVP+ level) or a transition state (at the B3LYP/CEP-31G level) with its energy being higher than the $^1\Sigma$ ground state by 12.4 and 6.4 kcal/mol, respectively, at the above two levels. For structure **6c**, when C_{2v} symmetry is constrained, it has an imaginary vibrational frequency. Following the eigenvector for the imaginary frequency leads to another Pb-capped C_6 monocyclic structure, in which all the seven atoms are still in a plane but the point group symmetry of the cluster is reduced form C_{2v} to C_s. This C_s symmetry structure is a minimum with its energy lying 34.2 kcal/mol above the $^1\Sigma$ ground state at the B3LYP/TZVP+ level of calculation. The kitelike structure with C_{2v} symmetry (**6d**) is also a minimum on the PES of PbC_6, but its relatively high energy, about 50 kcal/mol above the $^1\Sigma$ ground state, expresses that this structure should be less stable.

According to the calculations above, the PbC_n ($n\leqslant 6$) clusters mainly have linear structures with the Pb atom located at one end (**na**). On the other hand, when more C atoms are included, the Pb-containing $(n+1)$-membered monocyclic ring structure (**nb**) and the Pb-side-on C_n monocyclic ring structure (**nc**) also should have lower energies. Therefore, for PbC_7-PbC_{10} clusters, only these three kinds of structures are investigated. For the PbC_7 cluster, all of our calculations predict linear PbCCCCCCC structure (**7a**) in its triplet $^3\Sigma$ state has lowest energy and all real vibrational frequencies, indicating it should be the ground state of PbC_7. The singlet $^1\Delta$ state of **7a** is 9.1 kcal/mol energetically less stable at the B3LYP/TZVP+ level of theory. The calculated bond distances for the ground state structure are $R(\mathrm{Pb1-C2})=2.076$, $R(\mathrm{C2-C3})=1.268$, $R(\mathrm{C3-C4})=1.294$, $R(\mathrm{C4-C5})=1.273$, $R(\mathrm{C5-C6})=1.275$, $R(\mathrm{C6-C7})=1.293$, and $R(\mathrm{C7-C8})=1.287$ Å. For the Pb-containing monocyclic ring structure (**7b**) of PbC_7, its singlet $^1A_1$ state and triplet $^3B_1$ are energetically less stable than the $^3\Sigma$ ground state (**7a**) by 17.3 and 22.3 kcal/mol, respectively. For the Pb-side-on C_7 monocyclic structure (**7c**) of PbC_7, its singlet $^1A_1$ state has four imaginary vibrational frequencies and very high energy, and further calculations following the normal modes related to the imaginary frequencies do not reduce the energy dramatically. The triplet $^3B_1$ state of **7c** has all real vibrational frequencies with its energy 38.2 kcal/mol higher than that of the $^3\Sigma$ ground state (**7a**) at the B3LYP/TZVP+ level of computations.

The global minimum of the neutral PbC_8 cluster is also its linear PbCCCCCCCC isomer (**8a**). Its electronic ground state is the singlet $^1\Sigma$ state with the corresponding triplet $^3\Sigma$ state being higher in energy by 19.5 kcal/mol at the B3LYP/TZVP+ level of theory. The calculated bond distances for the global minimum are $R(\mathrm{Pb1-C2})=2.040$, $R(\mathrm{C2-C3})=1.264$, $R(\mathrm{C3-C4})=1.302$, $R(\mathrm{C4-C5})=1.256$, $R(\mathrm{C5-C6})=1.296$, $R(\mathrm{C6-C7})=1.258$, $R(\mathrm{C7-C8})=1.304$, and $R(\mathrm{C8-C9})=1.275$ Å. For Pb-containing monocyclic ring structure (**8b**) of PbC_8, when C_{2v} symmetry is constrained, structure **8b** in its lowest-lying $^1A_1$ state has two imaginary vibrational frequencies, indicating that structure **8b** is a saddle point on the PES of PbC_8. Following the eigenvectors for the imaginary frequencies leads to a C_1 symmetry nonplanar ring structure. Compared with the C_{2v} symmetry ring structure (**8b**), this nonplanar ring structure is 1.7 kcal/mol more stable, but it is still 20.9 kcal/mol less stable than the $^1\Sigma$ ground state (**8a**). Structure **8c** has two or more imaginary vibrational frequencies. Because of its too high energy, we do not consider it further.

The B3LYP/TZVP+ method predicts that neutral PbC_9 cluster has a linear PbCCCCCCCCC ground state structure (**9a**) with a triplet $^3\Sigma$ electronic state. The calculated bond distances for the linear structure **9a** in its $^3\Sigma$ state are $R(\mathrm{Pb1-C2})=2.074$, $R(\mathrm{C2-C3})=1.266$, $R(\mathrm{C3-C4})=1.298$, $R(\mathrm{C4-C5})=1.268$, $R(\mathrm{C5-C6})=1.282$, $R(\mathrm{C6-C7})=1.279$, $R(\mathrm{C7-C8})=1.271$, $R(\mathrm{C8-C9})=1.295$, and $R(\mathrm{C9-C10})=1.284$ Å. Compared with the $^3\Sigma$ state of **9a**, the Pb-containing 10-membered ring structure (**9b**) has lower energy at the B3LYP/CEP-31G level, but more reliable B3LYP/TZVP+ method predicts that structure **9b** (in its lowest-lying $^3B_1$ state) is 13.3 kcal/mol energetically much higher. Similarly, although the B3LYP/CEP-31G calculations give the Pb-side-on C_9 monocyclic structure (**9c**) in its singlet $^1A_1$ state has lowest energy among the structures investigated, the B3LYP/TZVP+ method predicts that this $^1A_1$ state is less stable than the $^3\Sigma$ state of **9a** by 7.6 kcal/mol.

Unlike the cases of PbC_n ($n\leqslant 9$), which all have the linear structures as their ground states, our calculations predict that, for neutral PbC_{10} cluster, the linear PbCCCCCCCCCC structure (**10a**) is less stable than the Pb-containing 11-membered ring structure (**10b**) or the Pb-side-on C_{10} monocyclic structure (**10c**). At the B3LYP/TZVP+ level, structure **10b** with C_{2v} symmetry in its singlet $^1A_1$ state has lowest energy and all real vibrational frequencies, indicating that it should be the global minimum of PbC_{10}. On the other hand, the B3LYP/CEP-31G calculations give the $^1A_1$ state of structure **10b** an imaginary vibrational frequency $(46.10i, b_2)$. Following the normal mode for the imaginary frequency leads to a similar 11-membered ring structure but the point group symmetry of the cluster is reduced from C_{2v} to C_s. This C_s symmetry ring structure is a minimum with its energy lying only 2.6 kcal/mol below the C_{2v} symmetry ring structure at the B3LYP/CEP-31G level of theory. It should be noted that this C_s symmetry ring structure goes back to the above C_{2v} symmetry ring structure (**10b**) when B3LYP/TZVP+ method is used. For the Pb-side-on C_{10} monocyclic structure, when C_{2v} symmetry is constrained, structure **10c** has an imaginary vibrational frequency. Further calculations following the normal mode of the imaginary frequency leads to a C_s symmetry structure (**10c-2**) with geometries of $R(\mathrm{Pb1-C2})=2.238$,

R(C2–C3)=1.431, R(C3–C4)=1.363, R(C4–C5)=1.243 Å, R(C5–C6)=1.339, R(C6–C7)=1.257, R(C7–C8)=1.328 Å, R(C8–C9)=1.272, R(C9–C10)=1.308, R(C10–C11)=1.263 Å, A(C2–C3–C4)=125.7, A(C3–C4–C5)=155.6, A(C4–C5–C6)=160.8, A(C5–C6–C7)=129.4, A(C6–C7–C8)=155.6, A(C7–C8–C9)=120.8, A(C8–C9–C10)=159.9, A(C9–C10–C11)=139.5°. Compared with the $^1A_1$ state of **10b**, structure **10c-2** in its $^1A'$ state is 0.3 kcal/mol less stable with the B3LYP/TZVP+ method while 4.6 kcal/mol more stable with the B3LYP/TZVP+ method.

In summary, for the neutral PbC_n clusters, when $n=1$, the PbC_1 cluster has a triplet $^3\Pi$ ground state; when $n=2$, the global minimum of PbC_2 is found by the B3LYP/CEP-31G and CCSD(T) calculations to have a Pb-terminated bent chain structure (**2b**) and a singlet $^1A'$ state; when $n=3-9$, the linear isomer having a terminal lead atom (**3a**, **4a**, **5a**, **6a**, **7a**, **8a**, **9a**) is the lowest energy form for every member of this PbC_n series and the electronic ground state is triplet $^3\Sigma$ for n-odd member or singlet $^1\Sigma$ for the n-even member; when $n=10$, the PbC_{10} cluster possesses a Pb-containing 11-membered ring ground state structure.

Removing an electron from neutral PbC_n gives cationic PbC_n^+ clusters. All the structures studied for PbC_n are also investigated for the PbC_n^+ cations. Both the doublet and the quartet electronic states are considered for each structure of PbC_n^+. As shown in Table I, all the PbC_n^+ clusters have doublet ground states except for PbC^+, which has a quartet $^4\Sigma$ ground state with a $\{\text{core}\}\sigma^2\sigma^2\sigma^1\pi^2$ valence electronic configuration. Similar to PbC_2, structure **2a**, **2b**, and **2c** have almost degenerate energies for the PbC_2^+ cluster cation. At the B3LYP/TZVP+ level, structure **2b** in its $^2A'$ state has lowest energy while structure **2c** in its $^2A_1$ state and structure **2a** in its $^2\Sigma$ state lie 0.1 and 0.6 kcal/mol above, respectively. The global minimum of the PbC_3^+ cluster cation has a $C_{\infty v}$ symmetry linear structure (**3a**) and a doublet $^2\Pi$ electronic state. This is also the case for the cationic PbC_5^+, PbC_7^+, PbC_8^+, and PbC_9^+ clusters, i.e., their global minima all have linear structures (**5a**, **7a**, **8a**, and **9a**) and $^2\Pi$ states. On the other hand, all of our calculations predict that, for the cationic PbC_4^+ and PbC_6^+ clusters, the $C_{\infty v}$ symmetry linear structures **4a** and **6a** in their doublet $^2\Pi$ states are transition states for they both have an imaginary vibrational frequency. Following the eigenvector for the imaginary frequency leads to a C_s symmetry quasilinear structure for PbC_4^+ and a C_1 symmetry quasilinear structure for PbC_6^+, which both possess all real vibrational frequencies. For PbC_4^+, the C_s symmetry quasilinear structure in its $^2A'$ state has lowest total energy, lying 0.9 kcal/mol below the linear structure **4a** ($^2\Pi$), indicating it should be the global minimum on the PES of PbC_4^+. For PbC_6^+, the C_1 symmetry quasilinear structure in its $^2A'$ state and the corresponding linear structure **6a** in its the $^2\Pi$ state have almost degenerate energies, with the former being only 0.1 kcal/mol energetically more stable. The optimized geometries are R(Pb1–C2)=2.129, R(C2–C3)=1.251, R(C3–C4)=1.322, R(C4–C5)=1.282 Å, A(Pb1–C2–C3)=175.4, A(C2–C3–C4)=177.3, A(C3–C4–C5)=164.0° for the C_s symmetry quasi-linear structure of PbC_4^+, and R(Pb1–C2)=2.119, R(C2–C3)=1.251, R(C3–C4)=1.314, R(C4–C5)=1.255, R(C5–C6)=1.300, R(C6–C7)=1.296 Å, A(Pb1–C2–C3)=179.5, A(C2–C3–C4)=179.9, A(C3–C4–C5)=179.9, A(C4–C5–C6)=179.4, A(C5–C6–C7)=170.0° for the C_1 symmetry quasilinear structure of PbC_6^+, respectively. For PbC_{10}^+ cation, the most stable isomer possesses a Pb-side-on C_{10} monocyclic structure with C_s symmetry (**10c-2**) while the linear $(PbCCCCCCCCCC)^+$ structure in its $^2\Pi$ state is 4.2 and 14.4 kcal/mol higher at the B3LYP/TZVP+ and B3LYP/CEP-31G levels, respectively. The optimized geometries for structure **10c-2** are R(Pb1–C2)=2.290, R(C2–C3)=1.405, R(C3–C4)=1.328, R(C4–C5)=1.267 Å, R(C5–C6)=1.298, R(C6–C7)=1.278, R(C7–C8)=1.295 Å, R(C8–C9)=1.283, R(C9–C10)=1.294, R(C10–C11)=1.271 Å, A(C2–C3–C4)=128.0, A(C3–C4–C5)=158.2, A(C4–C5–C6)=151.5, A(C5–C6–C7)=137.1, A(C6–C7–C8)=151.2, A(C7–C8–C9)=125.4, A(C8–C9–C10)=157.7, A(C9–C10–C11)=137.1°. The Pb-side-on C_{10} monocyclic structure with C_{2v} symmetry (**10c**) has one imaginary vibrational frequency.

Attaching an electron to neutral PbC_n gives anionic PbC_n^- clusters. Again, we choose all the structures considered for PbC_n as the initial structures of the PbC_n^- anions, and both the doublet and the quartet electronic states are investigated for each structure of the PbC_n^- clusters. The computational results for the PbC_n^- clusters are also given in Tables I and II. The electronic ground state of the PbC^- anion has $^2\Sigma$ symmetry and a $\{\text{core}\}\sigma^2\sigma^2\sigma^1\pi^4$ valence electronic configuration. For each PbC_n^- ($n=2-10$) cluster, the $C_{\infty v}$ symmetry linear structure (**na**) in its $^2\Pi$ state has all real vibrational frequencies and the lowest energy, expressing that it should be the global minimum on the corresponding potential energy hypersurface.

B. Stabilities

To compare the relative stability of the clusters with different sizes, we adopt the concept of incremental binding energy,[21–25,79] labeled as ΔE^L, as suggested by Pascoli and Lavendy. ΔE_n^L is defined as the consecutive binding energy difference between adjacent $PbC_n/PbC_n^+/PbC_n^-$ and $PbC_{n-1}/PbC_{n-1}^+/PbC_{n-1}^-$ clusters, and can be determined by the reaction energies of

$$PbC_n \rightarrow PbC_{n-1} + C_1, \quad \text{(DN1)}$$

$$PbC_n^+ \rightarrow PbC_{n-1}^+ + C_1, \quad \text{(DC2)}$$

$$PbC_n^- \rightarrow PbC_{n-1}^- + C_1. \quad \text{(DN3)}$$

The incremental binding energies versus the carbon atom numbers for Pb-doped linear carbon clusters $PbC_n/PbC_n^+/PbC_n^-$ are presented in Fig. 2. From Fig. 2 we can see that there exists a strong even–odd alternation in the cluster stability for neutral PbC_n and anionic PbC_n^-, with their n-even members being much more stable than the corresponding odd $n-1$ and $n+1$ ones, while for cationic PbC_n^+ clusters, the parity effect is very weak.

Systematical investigations on second-row-atom-doped linear carbon clusters[80] have shown that, for linear

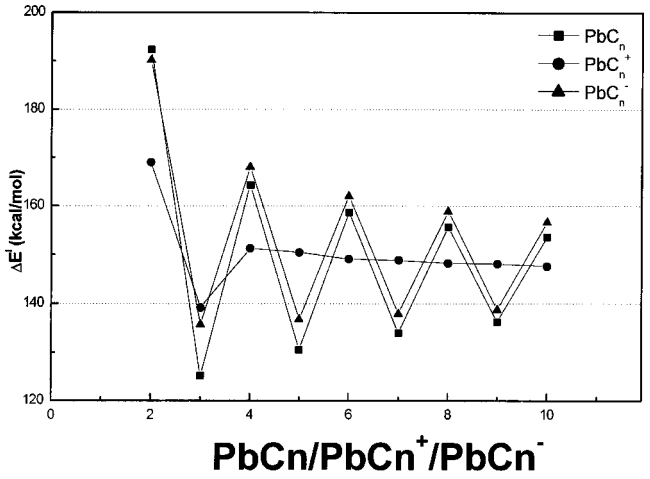

FIG. 2. Incremental binding energies for linear $PbC_n/PbC_n^+/PbC_n^-$ clusters vs the number of carbon atoms.

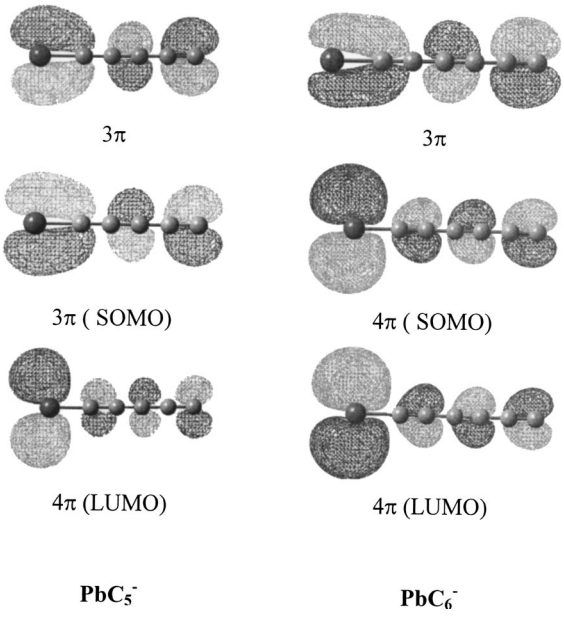

FIG. 3. The highest fully occupied molecular orbital (HFOMO), the singly occupied molecular orbital (SOMO), and the lowest unoccupied molecular orbital (LUMO) of linear PbC_5^- and PbC_6^- clusters. The core orbitals, formed by the $1s$ orbitals of the carbon atoms and the $1s2s2p3s3p3d4s4p4d4f5s5p5d$ orbitals of the lead atom, are excluded and not numbered herein.

$C_nX/C_nX^+/C_nX^-$ ($n=1-10$, X=Na, Mg, Al, Si, P, S, or Cl), the parity effect in cluster relative stability is a result of the number of available valence π-electrons, especially the electron number in π-type highest occupied molecular orbital (HOMO). Similar to linear SiC_n, when the core $1s^2$ electrons for each carbon atom and $1s^22s^22p^63s^23p^63d^{10}4s^24p^64d^{10}4f^{14}5s^25p^65d^{10}$ electrons for lead atom are excluded, linear PbC_n has $4n+4$ valence electrons, and the electronic configurations can be summarized as followed:

$$(\text{core})1\sigma^2\cdots 1\pi^4\cdots(n+2)\sigma^2\left(\frac{n}{2}\right)\pi^4,$$

n-even members,

$$(\text{core})1\sigma^2\cdots 1\pi^4\cdots(n+2)\sigma^2\left(\frac{n+1}{2}\right)\pi^2,$$

n-odd members (except for PbC).

Thus, except for the smallest member PbC, linear PbC_n cluster contains $2n+4$ valence σ-electrons and $2n$ valence π-electrons. The $2n+4$ σ-electrons fully occupy $n+2$ σ-orbitals. For the species with even n, the $2n$ π-electrons constitute a closed shell, resulting in a $\cdots\pi^4$ electronic configuration and a $^1\Sigma$ state, while for the cluster with odd n, the π-type HOMO is half-filled with only two electrons, resulting in a $\cdots\pi^2$ electronic configuration and a $^3\Sigma$ state. Since the former situation (fully filled π-orbitals) is energetically much more stable than the latter one (half-filled π-orbitals), a strong even–odd alternation exists in the stability of linear PbC_n clusters, with the n-even members being much more stable than the n-odd ones. Cationic PbC_n^+ has one less valence electron than neutral PbC_n. For linear PbC_n^+, its n-even member has a $\cdots\pi^1$ electronic configuration and its n-odd member has a $\cdots\pi^3$ electronic configuration. None of them correspond to a fully filled HOMO, so the stabilities for both n-odd and n-even species do not differ much.

It is very interesting to note that, for linear PbC_n^- anions, the "valence π-electrons number" rule—it is the number of available valence π-electrons that determines the relative stabilities of the heteroatom-doped linear carbon clusters—is invalid. Anionic PbC_n^- has one more valence electron than neutral PbC_n. Linear PbC_n^- has $\cdots\pi^1$ electronic configuration for its n-even member and $\cdots\pi^3$ electronic configuration for its n-odd member. Again, none of them corresponds to a fully filled HOMO, so the parity effect for linear PbC_n^- should also less pronounced, according to the "valence π-electrons number" rule. However, this is not the case. To understand the origin of this conflict, Fig. 3 displays the valence molecular orbitals of linear PbC_5^- and PbC_6^- cluster. For linear PbC_5^- anion, the singly occupied molecular orbital (SOMO) is a π-type bond orbital, while the SOMO of linear PbC_6^- anion is best described as π-type lone-pair orbital. When going from PbC_5^- to PbC_6^-, one electron will occupy π-type bond orbital. On the other hand, when going from PbC_6^- to PbC_7^-, both the two π electrons will occupy π-type lone-pair orbitals. These are also the cases for other PbC_n^- anions. Perhaps this is the reason why the n-even members of the PbC_n^- anions are much more stable than the corresponding odd $n-1$ and $n+1$ ones. The theoretical result predicted herein is in good agreement with the even–odd alternation mass distribution observed in our recent time-of-flight mass spectra (Fig. 4).

C. Ionization potentials and electron affinities

Comparing the total energies of PbC_n, PbC_n^+, and PbC_n^-, we get the ionization potential (IP) and the electron affinities (EA) of the PbC_n clusters. Three forms of the ionization potential are reported herein, evaluated as the difference of total energies in the following manner:
the adiabatic ionization potential are determined by

$$\text{IP}_{\text{ad}}=E(\text{optimized cation})-E(\text{optimized neutral}),$$

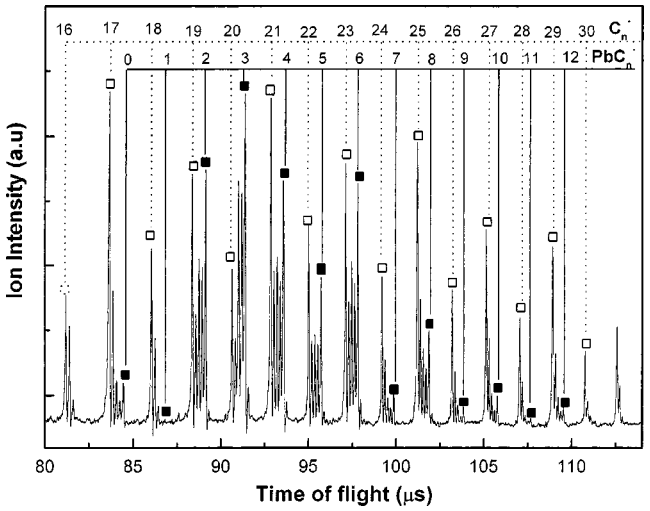

FIG. 4. Time-of-flight mass spectrum of PbC_n^- produced by laser ablating the mixture of lead and carbon powders. Details of the experimental setup have been described in the previous paper (Ref. 81). Briefly, the clusters were produced by direct laser ablation (532 nm output of a pulsed YAG laser, about 10 mJ/Pulse) on a target plate. The plume expanded into a high vacuum chamber with an operating pressure of about 10^{-6} Torr, and no buffer gas was introduced during this experiment. Then they entered perpendicularly into the accelerating area and were analyzed by the reflection time-of-flight mass spectrometer. Dramatic even–odd alternation of the ion signal intensity of PbC_n^- can be observed except that of PbC_3^-.

the vertical electron affinity by

$$IP_{vert} = E(\text{cation at optimized neutral geometry}) - E(\text{optimized neutral}),$$

and the vertical ionization potential of the cation by

$$IP_{VAE} = E(\text{optimized cation}) - E(\text{neutral at optimized cation geometry}).$$

Since the total energy of the optimized cation, *E* (optimized cation), is lower than the total energy of the cation at the optimized neutral geometry, *E* (cation at optimized neutral geometry), and the total energy of the optimized neutral molecule, *E* (optimized neutral), is lower than the total energy of the neutral molecule at the optimized cation geometry, *E* (neutral at optimized cation geometry), three forms of EA should have an order of $IP_{VAE} < IP_{ad} < IP_{vert}$. Thus, for the IPs of any system, the IP_{VAE} gives the lower bound while the IP_{ver} gives the upper bound.

Similarly, there are also three forms of electron affinity, according to the following energy differences.

The adiabatic electron affinity are determined by

$$EA_{ad} = E(\text{optimized neutral}) - E(\text{optimized anion}),$$

the vertical electron affinity by

$$EA_{vert} = E(\text{optimized neutral}) - E(\text{anion at optimized neutral geometry}),$$

and the vertical detachment energy of the anion by

$$EA_{VDE} = E(\text{neutral at optimized anion geometry}) - E(\text{optimized anion}).$$

and an EA order of $EA_{vert} < EA_{ad} < EA_{VDE}$, with the EA_{vert} giving the lower bound and the EA_{VDE} giving the upper bound.

Figure 5 depicts the IP and EA values as function of the number of carbon atoms in the clusters. For the IPs of $PbC_n/PbC_n^+ (n=1-9)$, the IP_{ad}, IP_{vert}, and IP_{VAE} have similar values due to the small geometry changes between neutral PbC_n and its PbC_n^+ cations. The large geometrical difference between the global minima for PbC_{10} and PbC_{10}^+ leads to the IP_{VAE} value being much higher than the IP_{ad} and IP_{vert} values. For the EAs of PbC_n/PbC_n^-, when $n=1-9$, the EA_{ad}, EA_{vert}, and EA_{VDE} values are also similar because of the similar ground state structures between the neutral PbC_n and its corresponding PbC_n^- anions, which all have linear ground state structures. When $n=10$, the EA_{VDE} value is much lower than those of the EA_{ad} and EA_{vert} because the global minima for the neutral PbC_{10} and anionic PbC_{10}^- have significantly different geometries. On the other hand, there is an obvious even–odd parity effect in the ionization potential curve of PbC_n, *n*-even clusters having higher IP than *n*-odd ones. This behavior is related to the higher stability of *n*-even PbC_n clusters than the *n*-odd ones. It should be noted that, although the PbC_n^- anions have a strong even–odd alternation effect in cluster stabilities, the parity effect in the electron affinity curve is less pronounced, because neutral PbC_n have very similar alternation trends to anionic PbC_n^-. Thus, the statement that the even–odd alternation in the time-of-flight signal intensities is ascribed to the parity effect of the calculated EAs[17–19] is not always right. It is also easily seen in Fig. 5 that there is a tendency to lower IPs and higher EAs as *n* increases.

D. Fragmentation energies

Various fragmentation energies, as the function of the number of clustering carbon atoms, for linear $PbC_n/PbC_n^+/PbC_n^-$ clusters, are displayed in Fig. 6. Besides the fragmentation energies accompanying channel DN1, DC1, and DA1, many other dissociation reactions are also examined, which include the following seven channels for neutral PbC_n clusters:

$$PbC_n \rightarrow PbC_{n-2} + C_2, \quad \text{(DN2)}$$

$$PbC_n \rightarrow PbC_{n-3} + C_3, \quad \text{(DN3)}$$

$$PbC_n \rightarrow C_n + Pb, \quad \text{(DN4)}$$

$$PbC_n \rightarrow C_{n-1} + PbC, \quad \text{(DN5)}$$

$$PbC_n \rightarrow C_{n-2} + PbC_2, \quad \text{(DN6)}$$

$$PbC_n \rightarrow C_{n-3} + PbC_3, \quad \text{(DN7)}$$

$$PbC_n \rightarrow C_n^- + Pb^+; \quad \text{(DN8)}$$

the following 10 channels for cationic PbC_n^+ clusters:

$$PbC_n^+ \rightarrow PbC_{n-2}^+ + C_2, \quad \text{(DC2)}$$

$$PbC_n^+ \rightarrow PbC_{n-3}^+ + C_3, \quad \text{(DC3)}$$

$$PbC_n^+ \rightarrow PbC_n^+ + Pb, \quad \text{(DC4)}$$

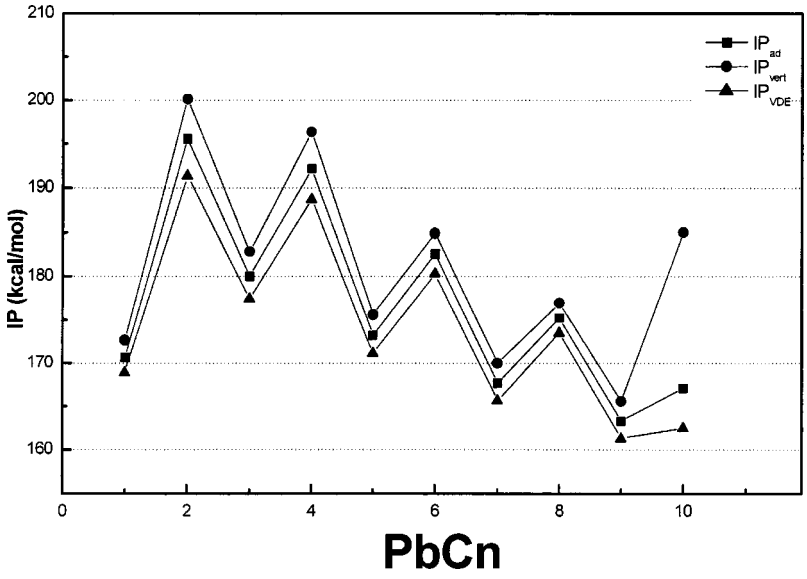

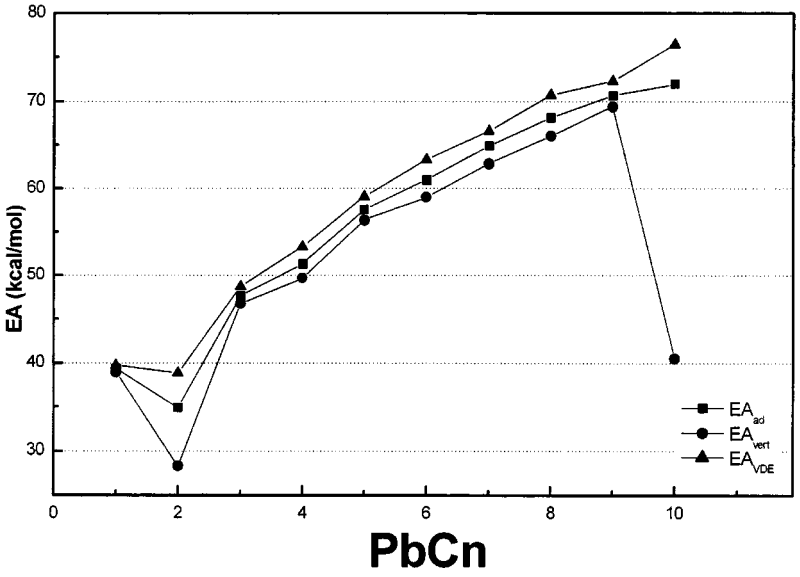

FIG. 5. Ionization potentials (IP) and electron affinities (EA) of PbC_n clusters vs the number of carbon atoms.

$$PbC_n^+ \rightarrow C_{n-1}^+ + PbC, \quad \text{(DC5)}$$

$$PbC_n^+ \rightarrow C_{n-2}^+ + PbC_2, \quad \text{(DC6)}$$

$$PbC_n^+ \rightarrow C_{n-3}^+ + PbC_3, \quad \text{(DC7)}$$

$$PbC_n^+ \rightarrow C_n + Pb^+, \quad \text{(DC8)}$$

$$PbC_n^+ \rightarrow C_{n-1} + PbC^+, \quad \text{(DC9)}$$

$$PbC_n^+ \rightarrow C_{n-2} + PbC_2^+, \quad \text{(DC10)}$$

$$PbC_n^+ \rightarrow C_{n-3} + PbC_3^+; \quad \text{(DC11)}$$

and the following 13 channels for anionic PbC_n^- clusters:

$$PbC_n^- \rightarrow PbC_{n-2}^- + C_2, \quad \text{(DA2)}$$

$$PbC_n^- \rightarrow PbC_{n-3}^- + C_3, \quad \text{(DA3)}$$

$$PbC_n^- \rightarrow PbC_{n-1} + C^-, \quad \text{(DA4)}$$

$$PbC_n^- \rightarrow PbC_{n-2} + C_2^-, \quad \text{(DA5)}$$

$$PbC_n^- \rightarrow PbC_{n-3} + C_3^-, \quad \text{(DA6)}$$

$$PbC_n^- \rightarrow C_n^- + Pb, \quad \text{(DA7)}$$

$$PbC_n^- \rightarrow C_{n-1}^- + PbC, \quad \text{(DA8)}$$

$$PbC_n^- \rightarrow C_{n-2}^- + PbC_2, \quad \text{(DA9)}$$

$$PbC_n^- \rightarrow C_{n-3}^- + PbC_3, \quad \text{(DA10)}$$

$$PbC_n^- \rightarrow C_n + Pb^-, \quad \text{(DA11)}$$

$$PbC_n^- \rightarrow C_{n-1} + PbC^-, \quad \text{(DA12)}$$

$$PbC_n^- \rightarrow C_{n-2} + PbC_2^-, \quad \text{(DA13)}$$

$$PbC_n^- \rightarrow C_{n-3} + PbC_3^-. \quad \text{(DA14)}$$

It should be noted that, in Fig. 6, the fragmentation energies of channel DN1, DC1, and DA1 are represented for comparison, while some channels with very high energies are excluded. From Fig. 6 we can see that losing a Pb atom is the

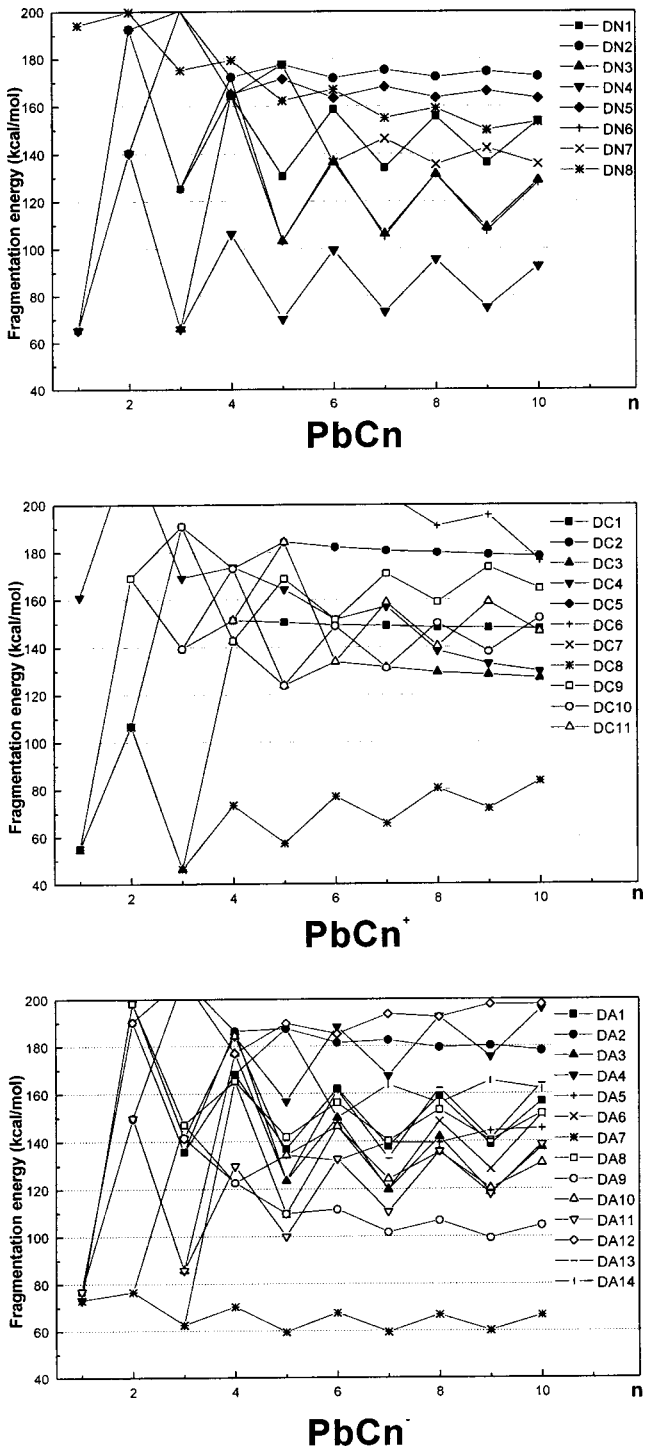

FIG. 6. Fragmentation energies of linear $PbC_n/PbC_n^+/PbC_n^-$ clusters. DNx, DAx, and DCx corresponds to different dissociation channels, as shown in the text.

dominant channel for neutral PbC_n (channel DN4) and anionic PbC_n^- (channel DA7), while for cationic PbC_n^+, the most favorable dissociation pathway is the loss of Pb^+ ion (channel DC8).

IV. CONCLUSION

Lead-doped carbon clusters PbC_n, PbC_n^+, and PbC_n^- have been simultaneously studied with DFT method at both B3LYP/CEP-31G and B3LYP/TZVP+level. The following conclusions have been reached:

(1) For neutral PbC_n clusters, when $n=1$, the PbC_1 cluster has a triplet $^3\Pi$ ground state; when $n=2$, the global minimum of PbC_2 has a Pb-terminated bent chain structure and a singlet $^1A'$ state; when $n=3-9$, the linear isomer having a terminal lead atom is the lowest energy form for every member of this series and the electronic ground state is triplet $^3\Sigma$ for n-odd member or singlet $^1\Sigma$ for the n-even member; when $n=10$, the cluster possesses a Pb-containing 11-membered ring ground state structure. All the PbC_n^+ clusters also have doublet ground states except for PbC^+, which has a quartet $^4\Sigma$ ground state. For PbC_2^+, the Pb-terminated bent structure in its $^2A'$ state has lowest energy. The global minimum for the PbC_3^+, PbC_5^+, PbC_7^+, PbC_8^+, and PbC_9^+ cations has $C_{\infty v}$ symmetry linear structure and doublet $^2\Pi$ electronic state, while that for PbC_4^+ and PbC_6^+ clusters has quasilinear structure. For PbC_{10}^+ cation, the most stable isomer possesses a Pb-side-on C_{10} monocyclic structure with C_s symmetry. The electronic ground state of the PbC^- anion has $^2\Sigma$ symmetry. For each PbC_n^- $(n=2-10)$ cluster, the $C_{\infty v}$ symmetry linear structure in its $^2\Pi$ state is the global minimum on the corresponding potential energy hypersurface.

(2) Strong even–odd alternations in the cluster stability exist for neutral PbC_n and anionic PbC_n^-, with their n-even members being much more stable than the corresponding odd $n-1$ and $n+1$ ones, while for cationic PbC_n^+ clusters, the alternation effect is less pronounced. The parity effect predicted by theoretical studies is in good agreement with the even–odd alternation mass distribution observed in our recent time-of-flight mass spectra.

(3) The parity effects in the cluster stability also reflect in the ionization potential and electron affinity curves.

(4) Losing a Pb atom is the dominant channel for neutral PbC_n and anionic PbC_n^-, while for cationic PbC_n^+, the most favorable dissociation pathway is the loss of Pb^+ ion.

ACKNOWLEDGMENTS

The authors thank colleagues in the State Key Laboratory of Molecular Reaction Dynamic for helpful discussions. Particular thanks go to Professor Laisheng Wang for supplying the $(5s5p1d/4s4p1d)$ basis set of lead atom. This research was supported by the National Natural Science Foundation of China (29890211, 20203020).

[1] W. Weltner, Jr. and R. J. Van Zee, Chem. Rev. **89**, 1713 (1989), and references cited therein.
[2] D. C. Parent and S. L. Anderson, Chem. Rev. **92**, 1541 (1992), and references cited therein.
[3] A. V. Orden and R. J. Saykally, Chem. Rev. **98**, 2313 (1998), and references cited therein.
[4] N. Moazzen-Ahmadi and F. Zerbetto, J. Chem. Phys. **103**, 6343 (1995).
[5] Z. Y. Liu, Z. C. Tang, R. B. Huang, Q. Zhang, and L. S. Zheng, J. Phys. Chem. A **101**, 4019 (1997).
[6] Z. C. Tang and J. J. BelBruno, Int. J. Mass. Spectrom. **208**, 7 (2001).
[7] T. F. Giesen, A. Van Orden, H. J. Hwang, R. S. Fellers, R. A. Provencal, and R. J. Saykally, Science **265**, 756 (1994), and references cited therein.
[8] N. Moazzen-Ahmadi, J. J. Thong, and A. R. W. McKellar, J. Chem. Phys. **100**, 4033 (1994), and references therein.
[9] R. J. Lagow, J. J. Kampa, H. C. Wei *et al.*, Science **267**, 362 (1995).
[10] M. Leleyter, Z. Phys. D: At., Mol. Clusters **12**, 381 (1989).
[11] R. B. Huang, C. R. Wang, Z. Y. Liu, L. S. Zheng, F. Qi, L. S. Sheng, S. Q. Yu, and Y. W. Zhang, Z. Phys. D: At., Mol. Clusters **33**, 49 (1995).

[12] C. R. Wang, R. B. Huang, Z. Y. Liu, and L. S. Zheng, Chem. Phys. Lett. **237**, 463 (1995).
[13] C. R. Wang, R. B. Huang, Z. Y. Liu, and L. S. Zheng, Chem. Phys. Lett. **242**, 355 (1995).
[14] Z. Y. Liu, R. B. Huang, Z. C. Tang, and L. S. Zheng, Chem. Phys. **229**, 335 (1998).
[15] J. J. Belbruno, Z. C. Tang, R. Smith, and S. Hobday, Mol. Phys. **99**, 957 (2001).
[16] A. Nakajima, T. Taguwa, K. Nakao, M. Gomei, R. Kishi, S. Iwata, and K. Kaya, J. Chem. Phys. **103**, 2050 (1995).
[17] C. G. Zhan and S. Iwata, J. Chem. Phys. **104**, 9058 (1996); **105**, 6578 (1996).
[18] C. G. Zhan and S. Iwata, J. Phys. Chem. A **101**, 591 (1997).
[19] C. G. Zhan and S. Iwata, J. Chem. Phys. **107**, 7323 (1997).
[20] M. Gomei, R. Kishi, A. Nakajima, S. Iwata, and K. Kaya, J. Chem. Phys. **107**, 10051 (1997).
[21] G. Pascoli and H. Lavendy, Int. J. Mass. Spectrom. **173**, 41 (1998).
[22] G. Pascoli and H. Lavendy, Int. J. Mass. Spectrom. **181**, 11 (1998).
[23] G. Pascoli and H. Lavendy, Int. J. Mass. Spectrom. **181**, 135 (1998).
[24] G. Pascoli and H. Lavendy, J. Phys. Chem. A **103**, 3518 (1999).
[25] H. Lavendy and G. Pascoli, Int. J. Mass. Spectrom. **189**, 125 (1999).
[26] G. Pascoli and H. Lavendy, Chem. Phys. Lett. **312**, 333 (1999).
[27] G. Pascoli and H. Lavendy, Int. J. Mass. Spectrom. **177**, 31 (1998).
[28] G. Pascoli and H. Lavendy, Int. J. Mass. Spectrom. **206**, 143 (2001).
[29] G. Pascoli and H. Lavendy, Eur. Phys. J. D **19**, 339 (2002).
[30] A. Largo, A. Cimas, P. Redondo, and C. Barrientos, Int. J. Quantum Chem. **84**, 127 (2001).
[31] A. Largo, P. Redondo, and C. Barrientos, J. Phys. Chem. A **106**, 4217 (2002).
[32] P. Thaddeus, S. E. Cummins, and R. A. Linke, Astrophys. J. **283**, L45 (1984).
[33] J. Cernicharo, C. A. Gottlieb, M. Guelin, P. Thaddeus, and M. Vrtilek, Astrophys. J. Lett. **341**, 25 (1989).
[34] M. Ohishi, N. Kaifu, K. Kawaguchi *et al.*, Astrophys. J. Lett. **345**, L83 (1989).
[35] G. Pascoli and M. Comeau, Astrophys. Space Sci. **226**, 147 (1995).
[36] P. Redondo, A. Saguillo, and A. Largo, J. Phys. Chem. A **102**, 3953 (1998).
[37] A. J. Apponi, M. C. McCarthy, C. A. Gottlieb, and P. Thaddeus, Astrophys. J. Lett. **516**, L103 (1999).
[38] D. L. Michalopoulos, M. E. Geusic, P. R. R. Langridge-Smith, and R. E. Smalley, J. Chem. Phys. **80**, 3556 (1984).
[39] R. S. Grev and H. F. Schaefer III, J. Chem. Phys. **80**, 3552 (1984).
[40] N. Moazzen-Ahmadi and F. Zerbetto, Chem. Phys. Lett. **164**, 517 (1989).
[41] I. L. Alberts, R. S. Grev, and H. F. Schaefer III, J. Chem. Phys. **93**, 5046 (1990).
[42] J. R. Flores and A. Largo, Chem. Phys. **140**, 19 (1990).
[43] D. C. Parent, Int. J. Mass Spectrom. Ion Processes **116**, 257 (1992).
[44] P. A. Withey and W. R. M. Graham, J. Chem. Phys. **96**, 4068 (1992).
[45] P. W. Deutsch and L. A. Curtiss, Chem. Phys. Lett. **226**, 387 (1994).
[46] C. M. L. Rittby, J. Chem. Phys. **100**, 175 (1994).
[47] J. D. Presilla-Marquez and W. D. M. Graham, J. Chem. Phys. **100**, 181 (1994).
[48] S. C. Ross, T. J. Butenhoff, E. A. Rohlfing, and C. M. Rohlfing, J. Chem. Phys. **100**, 4110 (1994).
[49] G. Froudakis, A. Zdetsis, M. Muhlhauser, B. Engels, and S. D. Peyerimhoff, J. Chem. Phys. **101**, 6790 (1994).
[50] A. Van Orden, T. F. Giesen, R. A. Provencal, H. J. Hwang, and R. J. Saykally, J. Chem. Phys. **101**, 10237 (1994).
[51] Q. J. Huang, Z. Y. Liu, H. F. Liu, R. B. Huang, and L. S. Zheng, Chin. J. Chem. Phys. **8**, 205 (1995).
[52] A. V. Orden, R. A. Provencal, T. F. Giesen, and R. J. Saykally, Chem. Phys. Lett. **237**, 77 (1995).
[53] Y. Negishi, A. Kimura, N. Kobayashi, H. Shiromaru, Y. Achiba, and N. Watanabe, J. Chem. Phys. **103**, 9963 (1995).
[54] T. Kimura, T. Sugai, and H. Shinohara, Chem. Phys. Lett. **256**, 269 (1996).
[55] S. Hunsicker and R. O. Jones, J. Chem. Phys. **105**, 5048 (1996).
[56] J. D. Presilla-Marquez, C. M. L. Rittby, and W. R. Graham, J. Chem. Phys. **106**, 8367 (1997).
[57] J. L. Fye and M. F. Jarrold, J. Phys. Chem. A **101**, 1836 (1997).
[58] M. C. McCarthy, A. J. Apponi, and P. Thaddeus, J. Chem. Phys. **110**, 10645 (1999).
[59] R. D. Cowan and D. C. Griffin, J. Opt. Soc. Am. **66**, 1010 (1976).
[60] J. P. Desclaux, Comput. Phys. Commun. **9**, 31 (1975).
[61] B. Metz, H. Stoll, and M. Dolg, J. Chem. Phys. **113**, 2563 (2000).
[62] G. Frenking, S. Fan, C. M. Marchand, and H. Grutzmacher, J. Am. Chem. Soc. **119**, 6648 (1997).
[63] X. Li, H. F. Zheng, L. S. Wang, A. E. Kuznetsov, N. A. Cannon, and A. I. Boldyrev, Angew. Chem. Int. Ed. Engl. **40**, 1867 (2001).
[64] M. Mian, N. M. Harrison, V. R. Saunders, and W. R. Flavell, Chem. Phys. Lett. **257**, 627 (1996).
[65] J. Muscat and C. Klauber, Surf. Sci. **491**, 226 (2001).
[66] D. G. Dai and K. Balasubramanian, J. Chem. Phys. **96**, 8345 (1992).
[67] D. G. Dai and K. Balasubramanian, Chem. Phys. Lett. **271**, 118 (1997).
[68] K. Balasubramanian and D. Majumdar, J. Chem. Phys. **115**, 8795 (2001).
[69] C. Y. Zhao and K. Balasubramanian, J. Chem. Phys. **116**, 10287 (2002).
[70] D. Becke, J. Chem. Phys. **98**, 5648 (1993).
[71] C. Lee, W. Yang, and R. G. Parr, Phys. Rev. B **37**, 785 (1988).
[72] W. J. Stevens, H. Basch, and M. Krauss, J. Chem. Phys. **81**, 6026 (1984).
[73] W. J. Stevens, M. Krauss, H. Basch, and P. G. Jasien, Can. J. Chem. **70**, 612 (1992).
[74] W. R. Wadt and P. J. Hay, J. Chem. Phys. **82**, 284 (1985).
[75] R. Krishnan, J. S. Binkley, R. Seeger, and J. A. Pople, J. Chem. Phys. **72**, 650 (1980).
[76] M. J. Frisch, G. W. Trucks, H. B. Schlegel *et al.*, GAUSSIAN 98, Revision A.9, Gaussian Inc., Pittsburgh, PA, 1998.
[77] G. D. Purvis III and R. J. Bartlett, J. Chem. Phys. **76**, 1910 (1982).
[78] K. Raghavachari, G. W. Trucks, J. A. Pople, and M. Head-Gordon, Chem. Phys. Lett. **157**, 479 (1989).
[79] K. Raghavachari and J. S. Binkley, J. Chem. Phys. **87**, 2191 (1987).
[80] G. L. Li and Z. C. Tang (unpublished).
[81] X. P. Xing, Z. X. Tian, P. Liu, Z. Gao, Q. H. Zhu, and Z. C. Tang, Chin. J. Chem. Phys. **15**, 83 (2002).